Hybrid fiber/bulk DIAL-Doppler lidar for CO2 and wind measurement at 2.05 μm

Mathys Thiers, Julien Lahyani, Nicolas Cézard, Fabien Gibert

Hybrid fiber/bulk DIAL-Doppler lidar for CO_2 and wind measurement at 2.05 µm

Mathys Thiers[(a)], Julien Lahyani[(a)], Nicolas Cézard[(b)], Fabien Gibert [(c)]

[(a)] DOTA, ONERA, Université Paris Saclay, F-91123 Palaiseau, France
[(b)] DOTA, ONERA, Université de Toulouse, F-31055 Toulouse, France
[(c)] Laboratoire de Météorologie Dynamique (LMD), Centre de Recherche National Scientifique (CNRS), Ecole Polytechnique, FR-91128 Palaiseau Cedex, France
Lead Author e-mail address: mathys.thiers@onera.fr

Abstract: We report on the development of a DIfferential Absorption Lidar (DIAL) with coherent detection using a hybrid fiber/bulk laser for CO_2 and wind measurement at 2.05 µm. Peak power is limited at 0.6 kW by Stimulated Brillouin Scattering in the fibered part. A Ho:YLF bulk amplifier allows to overcome this limitation, providing 12-19 dB additional gain depending on the pulse repetition frequency. The hybrid fiber/bulk architecture delivers laser pulses of 1.5 mJ, 200 ns at 20 kHz (30 W average power). The architecture provides easy tunability on pulse repetition frequency, duration, and wavelength emission around the absorption line. This flexibility allows for the adjustment of the compromise between measurement range and precision. Firsts measurements of CO_2 Volume Mixing Ratio (VMR) and wind speed are currently being carried out. Then, the system will be used to measure CO_2 emissions from thermal plants and atmospheric CO_2 fluxes using eddy covariance calculations.

1. Introduction

Carbon dioxide (CO_2) is the most important anthropogenic greenhouse gas contributing to global warming. It is important to evaluate precisely CO_2 fluxes emitted by industrial sites. Monitoring natural CO_2 fluxes between the atmosphere and ecosystems is also of interest to understand their response to global warming.

Differential Absorption Lidar (DIAL) enables range-resolved profiling of CO_2 in the atmosphere. Coherent detection allows additional measurement of the wind speed. The combination of gas and wind speed measurements can lead to CO_2 flux estimation [1,2].

Many CO_2 DIAL systems use lasers operating at 1.57 µm or 2.05 µm due to well-suited absorption line with appropriated cross-section, low temperature dependence, and weak interference with water vapor absorption [3]. The laser presented here operates at 2.05 µm to take advantage of the high absorption R30-line, thereby enhancing the sensitivity of lidar measurements. Additionally, highly efficient amplification is achievable in this spectral region using Ho:YLF crystals[4]. The lidar features an all fiber Master Oscillator Power Amplifier (MOPA) architecture followed by a single pass Ho:YLF bulk amplifier. This hybrid fiber/bulk architecture combines the robustness of fiber architecture and high peak power attainable in bulk material. The architecture offers a flexibility on the setting of the wavelength and the laser pulse repetition frequency (PRF). This flexibility makes the lidar suitable for both anthropogenic and natural CO_2 flux measurements. Natural fluxes monitoring requires quick measurements to resolve atmospheric turbulences [1]. For anthropogenic fluxes it could be worthy to decrease the measurement rate to increase the signal power per measurement. The flexibility on the wavelength enables to decrease the CO_2 absorption in case of highly concentrated CO_2 plumes. The lidar presented here operates at PRF ranging between 2 kHz and 20 kHz, making it sufficiently fast for measuring natural fluxes. The flexibility provided by the architecture is expected to allow for optimization of measurements in various scenarios of anthropogenic fluxes, depending on the size, distance and concentration of CO_2 plumes.

2. Experimental Set-up

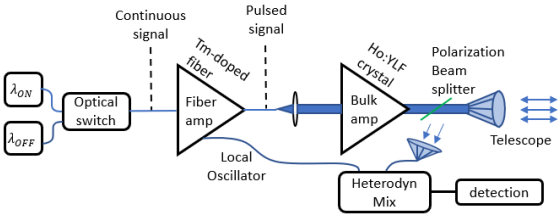

Figure 1 : Schematic view of the lidar with the hybrid emitter

Figure 1 presents the lidar architecture. The emitter is described in details in [5]. It uses two laser diodes to seed the MOPA chain with the two wavelengths λ_{ON} and λ_{OFF} used for DIAL measurements. An optical switch sequentially seeds the two laser diodes beams to the amplification chain, so that the emitter alternates the wavelength shot by shot. The continuous wave laser diode output is shaped into 200 ns pulses in the fibered architecture with an acousto-optic modulator. Peak power of the fibered part is limited at 0.6 kW by Stimulated Brillouin Scattering (SBS). The bulk amplifier allows to overcome this limitation. It features a Ho:YLF crystal pumped with a cw laser of 50 W with a wavelength of 1940 nm. The pump beam and the signal beam are combined and then separated with dichroic plates. They are focused in the crystal with a diameter of 0.6 mm. A monostatic telescope emits the pulses and collects the atmospheric backscattered signal.

The pulses energy at the output of the amplification depends of the pulse repetition frequency (PRF) as shown on Figure 2. A lower PRF enables the bulk amplifier to accumulate more gain resulting in more powerful pulses. The pulse energy at the output of the amplification chain is 1.5 mJ for a PRF of 20 kHz. The maximum pulse energy achievable with the emitter is 8 mJ at 2 kHz.

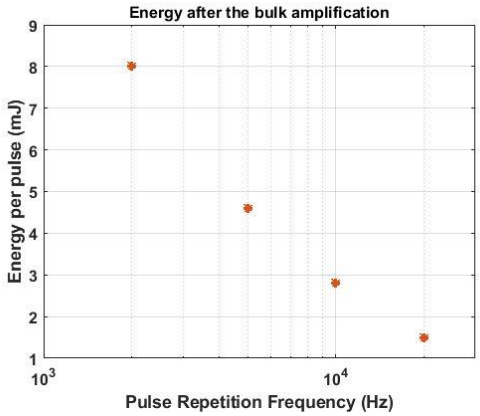

Figure 2 : Pulse energy as function of the PRF

The spatial quality of the emitted laser has been measured, since it is an essential parameter for coherent detection. It is characterized by the M^2 factor, and its value has been measured at 1.2, which corresponds to a loss of 20 % on the useful coherent signal (after interference with the single-mode beam of the local oscillator) [5]. The detector has a Noise Equivalent Power (NEP) of 8 pW/$\sqrt{\text{Hz}}$. With a local oscillator of 0.7 mW, the detection of the system is not fully limited by shot noise resulting in a degradation of the useful signal of 25% compared to the optimal shot-noise-limited value.

Table 1. Important parameters for CO_2 and wind measurements

Symbol	Parameter	Value
λ	Wavelength	2051 nm
PRF	Pulse repetition frequency	20 kHz
τ	Pulse duration	200 ns
E	Pulse energy	1.5 mJ
M^2	Beam quality factor	1.2
P_{OL}	Local Oscillator power	0.7 mW
NEP	Noise equivalent power	8 pW/$\sqrt{\text{Hz}}$
Φ_p	Pupil diameter	76 mm
T	Two-ways telescope transmission	0.6

3. Lidar applications

3.1. Simulations

The received backscattered power P_{ON} and P_{OFF} respectively for λ_{ON} and λ_{OFF}, are estimated with

the coherent detection. Then, the CO_2 volume mixing ratio (VMR) of an atmospheric layer located at a distance z with a thickness of Δz is calculated with the equation [1]:

$$VMR(z) = \frac{1}{2WF(z)\Delta z}\ln\left(\frac{P_{OFF}\left(z+\frac{\Delta z}{2}\right)}{P_{ON}\left(z+\frac{\Delta z}{2}\right)}\frac{P_{ON}\left(z-\frac{\Delta z}{2}\right)}{P_{OFF}\left(z-\frac{\Delta z}{2}\right)}\right) \quad (1)$$

Where WF is the weighting function (i.e, the difference of the cross section of the CO_2 at λ_{ON} and λ_{OFF}). The VMR random error is determined by the statistics of the estimation of backscattered power which is affected by speckle noise, shot noise, the Relative Intensity Noise of the local oscillator and the NEP of the detector. The Carrier-to-Noise Ratio (CNR) characterizes the quality of the heterodyne signal, and determines the random error on VMR estimation. With i_{het} the photocurrent associated to the heterodyne signal and i_{noise} the noise of the signal, and the brackets indicating the average, the CNR is:

$$CNR = \frac{<i_{het}^2>}{<i_{noise}^2>} \quad (2)$$

With CNR_{ON} the CNR associated to the ON-line backscattered signal the random error on VMR estimation is: [1]

$$\sigma_{VMR} = \frac{1}{2.WF(z).\Delta z.\sqrt{N_{acc}}}\sqrt{1+\sqrt{\left(\frac{1}{CNR_{ON}}\right)^2+\left(\frac{1}{CNR_{OFF}}\right)^2}} \quad (3)$$

Where N_{acc} is the number of acquired measurements.

Figure 3 shows a computation of the expected precision on CO_2 measurements according to the parameters of the set-up. An unknown parameter is the backscattering coefficient of the atmosphere, which is essential to predict CNR. This parameter has been previously estimated at 9.10^{-8} $m.sr^{-1}$ through fitting real data [6].

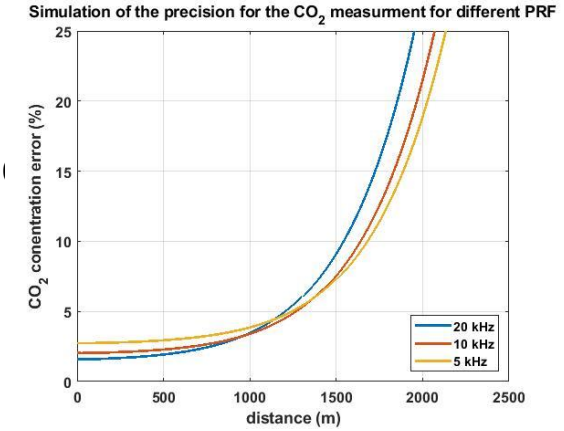

Figure 3 : Expected measurement performances with a collimated beam for a spatio-temporal integration of 90 m and 1 min

The simulation shows that a lower PRF increase the error at short range, and decreases the error at long range. Increasing the pulses energy is useless below 1000 m of range as the precision is limited by speckle noise, so the error increases as the data accumulation decreases. However, after 1000 m the increase of signal power improves the estimation precision. Selecting the appropriate PRF allows for maximizing the precision at short rang or at long-range depending on the area of interest.

3.2. Experiments

We have performed very recently our first lidar tests in the atmosphere. Figure 4 presents the CNR of the heterodyne signal, obtained in narrow band, with both the ON and OFF signal while horizontally probing of atmosphere. These signals were acquired the morning when the atmosphere contains a higher density of aerosols.

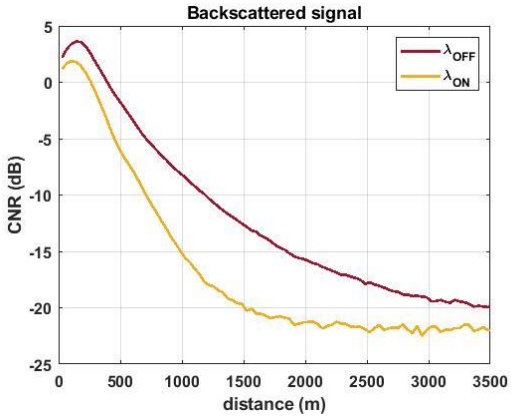

Figure 4 : First test with the lidar in the atmosphere. Spatio-temporal integration 30 m 1 min

The first measurements of CO_2 VMR and wind speed are currently being carried out.

4. Conclusion

The lidar DIAL-Doppler presented here has the versatility to be used as well for highly concentrated fluxes or for diffused fluxes carried by atmospheric turbulences. The freedom of setting the wavelength and the PRF allows for optimization of measurements in various scenario. Knowing the important parameters of the experimental set-up, it is possible to predict the performances of lidar measurements. The lidar is able to acquire atmospheric signal. A detailed study of the CO_2 and wind measurement performances is currently being carried out.

5. Perspectives

With incoming results of VMR and wind speed, we will assess the performances of lidar measurements, and compare them with the simulation presented in Figure 3

Our goal is then to enhance the setup by integrating a scanner to conduct 3D profiling of the atmosphere. This should enable us to estimate a CO_2 flux emitted from a thermal plant located in our university campus. Furthermore, we will evaluate the capability of the lidar to estimate atmospheric fluxes by using eddy covariance calculations.

6. References

[1] Gibert, F., Koch, G. J., Beyon, J. Y., Hilton, T. W., Davis, K. J., Andrews, A., Flamant, P. H., & Singh, U. N. (2011). “Can CO2 turbulent flux be measured by lidar? A preliminary study”. Journal of Atmospheric and Oceanic Technology Vol. 28, No. 3, 365-377 (2011).

[2] Yue, Bin, Saifen Yu, Manyi Li, Tianwen Wei, Jinlong Yuan, Zhen Zhang, Jingjing Dong, Yue Jiang, Yuanjian Yang, Zhiqiu Gao, and et al. 2022. "Local-Scale Horizontal CO2 Flux Estimation Incorporating Differential Absorption Lidar and Coherent Doppler Wind Lidar" Remote Sensing 14, no. 20: 5150 (2022)

[3] S. R. Kawa, J. B. Abshire, D. F. Baker, E. V. Browell, D. Crisp, S. M. R. Crowell, J. J. Hyon, J. C. Jacob, K. W. Jucks, B. Lin, R. T. Menzies, L. E. Ott, and T. S. Zaccheo, "Active Sensing of CO2 Emissions over Nights, Days, and Seasons (ASCENDS): Final Report of the ASCENDS," 228 (2018).

[4] Brian M. Walsh; Norman P. Barnes; Baldassare Di Bartolo. “Branching ratios, cross sections, and radiative lifetimes of rare earth ions in solids: Application to Tm^{3+} and Ho^{3+} ions in $LiYF_4$” J. Appl. Phys. 83, 2772–2787 (1998).

[5]Julien Lahyani, Mathys Thiers, Fabien Gibert, Dimitri Edouart, Julien Le Gouët, and Nicolas Cézard, “Hybrid fiber/bulk laser source designed for CO2 and wind measurements at 2.05 µm”. Optics Letters Vol. 49 Issue 4, 969-972 (2024).

[6] Julien Lahyani. « Lidar 2µm à source hybride fibrée/solide pour la télédétection du CO2 atmosphérique. » Physique. Institut Polytechnique de Paris, 2021